TLR4, TRIF, and MyD88 are essential for myelopoiesis and CD11c$^+$ adipose tissue macrophage production in obese mice

Received for publication, December 26, 2017, and in revised form, April 4, 2018 Published, Papers in Press, April 10, 2018, DOI 10.1074/jbc.RA117.001526

Cameron Griffin, Leila Eter, Nico Lanzetta, Simin Abrishami, Mita Varghese, Kaitlin McKernan, Lindsey Muir, Jamie Lane, Carey N. Lumeng, and Kanakadurga Singer[1]

From the Department of Pediatrics and Communicable Disease, University of Michigan Medical School, Ann Arbor, Michigan 48109

Edited by Jeffrey E. Pessin

Obesity-induced chronic inflammation is associated with metabolic disease. Results from mouse models utilizing a high-fat diet (HFD) have indicated that an increase in activated macrophages, including CD11c$^+$ adipose tissue macrophages (ATMs), contributes to insulin resistance. Obesity primes myeloid cell production from hematopoietic stem cells (HSCs) and Toll-like receptor 4 (TLR4), and the downstream TIR domain–containing adapter protein–inducing interferon-β (TRIF)- and MyD88-mediated pathways regulate production of similar myeloid cells after lipopolysaccharide stimulation. However, the role of these pathways in HFD-induced myelopoiesis is unknown. We hypothesized that saturated fatty acids and HFD alter myelopoiesis by activating TLR4 pathways in HSCs, differentially producing pro-inflammatory CD11c$^+$ myeloid cells that contribute to obesity-induced metabolic disease. Results from reciprocal bone marrow transplants (BMTs) with *Tlr4*$^{-/-}$ and WT mice indicated that TLR4 is required for HFD-induced myelopoiesis and production of CD11c$^+$ ATMs. Experiments with homozygous knockouts of *Irakm* (encoding a suppressor of MyD88 inactivation) and *Trif* in competitive BMTs revealed that MyD88 is required for HFD expansion of granulocyte macrophage progenitors and that *Trif* is required for pregranulocyte macrophage progenitor expansion. A comparison of WT, *Tlr4*$^{-/-}$, *Myd88*$^{-/-}$, and *Trif*$^{-/-}$ mice on HFD demonstrated that TLR4 plays a role in the production of CD11c$^+$ ATMs, and both *Myd88*$^{-/-}$ and *Trif*$^{-/-}$ mice produced fewer ATMs than WT mice. Moreover, HFD-induced TLR4 activation inhibited macrophage proliferation, leading to greater accumulation of recruited CD11c$^+$ ATMs. Our results indicate that HFD potentiates TLR4 and both its MyD88- and TRIF-mediated downstream pathways within progenitors and adipose tissue and leads to macrophage polarization.

Three decades of research have established the association among obesity, inflammation, and metabolic disease (1). Many of the associated co-morbidities of overnutrition in obese individuals (including insulin resistance, type 2 diabetes, atherosclerosis, cardiovascular disease, and some cancers) have been attributed to chronic low-grade inflammation, also known as meta-inflammation. More specifically, these obesity-induced diseases have been strongly correlated with an increase in myeloid leukocyte populations (macrophages and neutrophils) (2).

Obesity-induced alterations of tissue inflammatory macrophages, both in number and in activation state, have been directly associated with tissue dysfunction. Whereas local macrophage proliferation contributes to this accumulation (3), circulating pro-inflammatory Ly6c^{hi} monocyte populations are an important source of tissue macrophages (4). Ly6c^{hi} monocytes polarize and traffic into adipose tissue, giving rise to CD11c$^+$ macrophages, specifically in the visceral white adipose tissue (WAT)[2] of obese individuals (5). CD11c$^+$ adipose tissue macrophages (ATMs) are distinguished by a CD64$^+$/CD11c$^+$ phenotype in murine models and a CD206$^+$/CD11c$^+$ phenotype in humans and are recruited through chemokines and adipocyte signals that promote chemotaxis of monocytes (6–11). CD11c$^+$ ATMs accumulate disproportionately in visceral WAT and form ring structures known as crown-like structures (CLS) around damaged adipocytes in obese individuals. In contrast, CD11c$^-$, anti-inflammatory resident macrophages predominate in lean individuals (4). The presence of CLS is indicative of a pro-inflammatory state, as these macrophages have been found to secrete cytokines such as tumor necrosis factor-α and interleukin-1β (12) and are thus important contributors to

This work was supported by the University of Michigan Department of Pediatrics Janette Ferrantino Investigator Award; NIDDK, National Institutes of Health, Grant K08DK101755; and Edith Briskin/SKS Foundation Taubman Emerging Scholar support (to K. S.); National Institutes of Health Grants DK090262 (to C. N. L.); and National Institutes of Health Grant F32DK105676 (to L. M.). The authors declare that they have no conflicts of interest with the contents of this article. The content is solely the responsibility of the authors and does not necessarily represent the official views of the National Institutes of Health.

This article contains Figs. S1–S4.

[1] To whom correspondence should be addressed. Dept. of Pediatrics and Communicable Diseases, Division of Pediatric Endocrinology, D1205 MPB, 1500 E. Medical Center Dr., Ann Arbor, MI 48109. Tel.: 734-764-5175; Fax: 734-615-3353; E-mail: ksinger@umich.edu.

[2] The abbreviations used are: WAT, white adipose tissue; ATM, adipose tissue macrophage; HSC, hematopoietic stem cells; TLR, Toll-like receptor; TRIF, TIR domain–containing adapter–inducing interferon-β; MyD88, myeloid differentiation primary response 88; IRAKM, interleukin-1 receptor–associated kinase-M; cfu, colony-forming unit(s); HFD, high-fat diet; ND, normal diet; PA, palmitic acid; GWAT, gonadal white adipose tissue; IWAT, inguinal white adipose tissue; GM, granulocyte macrophage; APC, allophycocyanin; CLS, crown-like structures; LPS, lipopolysaccharide; BMT, bone marrow transplant; FFA, free fatty acid; DC, dendritic cell; BM, bone marrow; SVF, stromal vascular fraction.

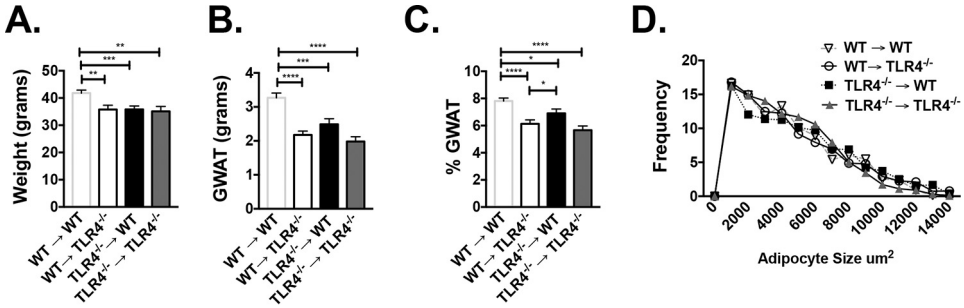

Figure 1. Reciprocal BMTs demonstrate that hematopoietic *Tlr4*$^{-/-}$ animals respond to high-fat diet. WT and *Tlr4*$^{-/-}$ C57Bl6/J male mice were irradiated at 8 weeks of age and then transplanted with marrow of the opposite genotype: WT marrow into *Tlr4*$^{-/-}$ (WT→*Tlr4*$^{-/-}$) *versus Tlr4*$^{-/-}$ marrow into WT mice (*Tlr4*$^{-/-}$→WT), with appropriate WT→WT and *Tlr4*$^{-/-}$→*Tlr4*$^{-/-}$ controls. 6 weeks after BMT, animals were started on HFD and assessed after 16 weeks for weight (*A*), GWAT weight (*B*), percentage GWAT (*C*), and GWAT adipocyte cross-sectional area distribution at 16 weeks of HFD (*D*). *, $p < 0.05$; **, $p < 0.01$; ***, $p < 0.005$; ****, $p < 0.001$. $n = 6–8$ in WT→WT and *Tlr4*$^{-/-}$→*Tlr4*$^{-/-}$ and $n = 10–14$ in WT→*Tlr4*$^{-/-}$ and *Tlr4*$^{-/-}$→WT groups. *Error bars*, S.E.

metabolic syndrome, specifically in visceral adipose tissue of males (13).

Given that the associated cytokines produced by ATMs mimic the inflammation from lipopolysaccharide (LPS) stimulation (14, 15), the Toll-like receptor 4 (TLR4) pathway has been implicated in obesity-induced inflammation. TLR complexes recognize pathogen-associated molecular patterns and signal via either an MyD88-dependent or -independent pathway (12). Downstream of TLR4, the MyD88 pathway activates the early phase of NF-κB, whereas the MyD88-independent or TRIF pathway activates interferon-regulatory factor (IRF3) and the late phase of NF-κB activation (16). NF-κB activation plays a key role in the regulation of both innate and adaptive immunity and consequently has been the target for many anti-inflammatory interventions. The role of TLR4 in the context of diet-induced adipose tissue inflammation and metabolic dysfunction is still unclear. Some investigators have reported a metabolic and inflammatory role for TLR4 (17, 18), whereas others have reported that TLR4 knockout does not improve metabolic function (19). The relative contribution of TRIF and MyD88 pathways to TLR4-mediated obesity–induced metabolic impairments and inflammation is unknown.

Whereas it has been shown that in obesity TLR4 deficiency significantly promotes alternative macrophage activation (19) and adipose tissue fibrosis (20), recent work in our laboratory demonstrated an additional role for TLR4 in the expansion of hematopoietic stem cells (HSCs) in obesity (2) and a role for MyD88 in the generation of myeloid progenitors in obesity. TLR4 activation in differentiated ATMs with fatty acids (17) in a high-fat diet environment is one possible mechanism explaining macrophage polarization, but a second mechanism of fatty acid activation within the hematopoietic progenitor cells probably exists as well.

There is a paucity of information on the possible dual role for TLR4, TRIF, and MyD88 pathways in hematopoietic precursors and in mature tissue macrophages. Therefore, we chose to investigate these pathways together in the context of diet-induced obesity. This is critical to understand, as interventions on these inflammatory pathways probably play a role in both the generation of myeloid cells and the activation profile of macrophages in obesity. Based on the literature and prior studies, we sought to evaluate the hypothesis that TLR4, TRIF, and MyD88 are required for hematopoietic stem and progenitor cell responses and tissue macrophage activation with obesity. Studies were carried out using hematopoietic knockout models and *in vivo* and *in vitro* assays of progenitor and macrophage activation to determine the contribution of TLR4, TRIF, and MyD88 pathways to diet-induced inflammation. We demonstrate that these pathways contribute significantly to production of CD11c$^+$ ATMs and myelopoiesis during HFD challenge.

Results

Hematopoietic-specific TLR4 knockout animals have reduced meta-inflammation compared with WT animals after HFD challenge

Whereas prior studies have demonstrated that hematopoietic *Tlr4*$^{-/-}$ mice have improved metabolism (18), it is unclear whether TLR4 deficiency has a direct impact on myeloid cell induction. Because it has been demonstrated that *Tlr4*$^{-/-}$ animals have fewer activated CD11c$^+$ ATMs with HFD (19), we sought to assess whether the production of CD11c$^+$ ATMs depended upon hematopoietic TLR4 expression by generating bone marrow transplant (BMT) chimeras. Young WT and *Tlr4*$^{-/-}$ animals were irradiated and given BM of the opposite genotype, generating WT→*Tlr4*$^{-/-}$ and *Tlr4*$^{-/-}$→WT animals. Control animals included WT→WT and *Tlr4*$^{-/-}$→*Tlr4*$^{-/-}$. 6 weeks after BMT, animals were started on HFD. After 16 weeks of HFD, WT→WT animals were heavier, but there were no differences in weight between the reciprocal groups (WT→*Tlr4*$^{-/-}$ and *Tlr4*$^{-/-}$→WT) (Fig. 1*A*). The same pattern was seen with gonadal white adipose tissue (GWAT) weight (Fig. 1*B*), but the percentage of GWAT per whole-body weight was higher in *Tlr4*$^{-/-}$→WT animals (Fig. 1*C*) compared with *Tlr4*$^{-/-}$ recipient animals. Subcutaneous inguinal white adipose tissue (IWAT) and liver weights were similar in all groups (Fig. S1, *A–C*), whereas spleen weights were slightly higher in WT recipient animals (WT→WT and *Tlr4*$^{-/-}$→WT (Fig. S1*D*). Although average adipocyte size was not different in the GWAT of both groups, there was a shift toward larger adipocytes in animals with *Tlr4*$^{-/-}$ marrow (Fig. 1*D*). These findings suggest that TLR4 deficiency in either BM or non-BM cells impairs HFD response, as demonstrated by differences in weight gain and adiposity.

To determine the impact of hematopoietic TLR4 on metabolism, animals were assessed throughout the course of HFD. At

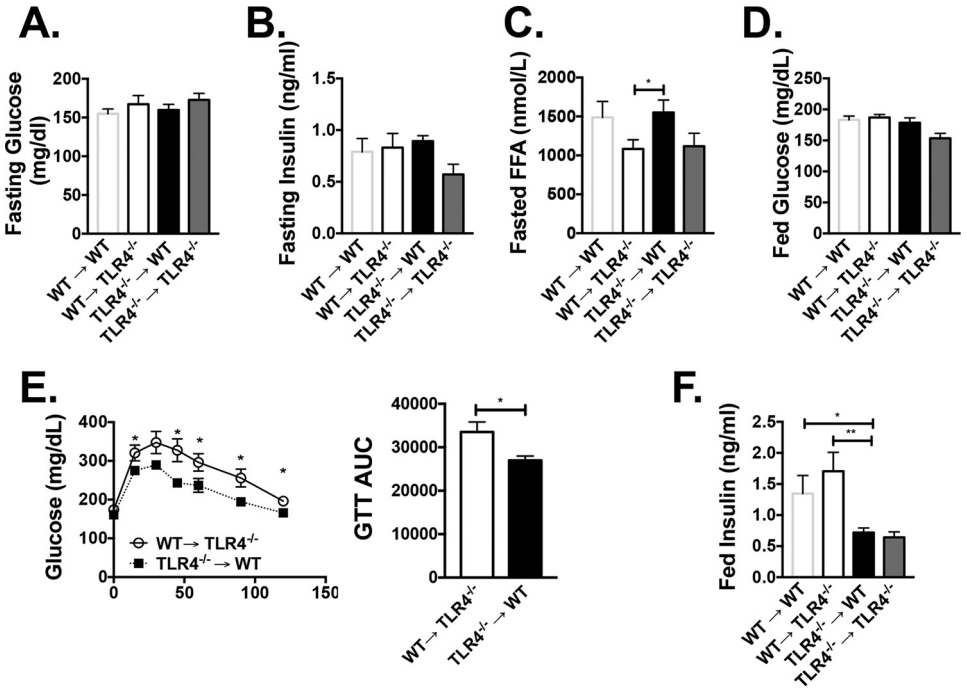

Figure 2. Hematopoietic *Tlr4*$^{-/-}$ animals have improved glucose tolerance. Metabolic assessments were performed on WT→*Tlr4*$^{-/-}$, *Tlr4*$^{-/-}$→WT animals, and controls. Fasting glucose (*A*), fasting insulin levels (*B*), and fasting FFAs (*C*) were measured after 10 weeks of HFD. *D*, fed glucose levels at 16 weeks of HFD. *E*, glucose tolerance testing in WT→*Tlr4*$^{-/-}$ and *Tlr4*$^{-/-}$→WT animals after 12 weeks of HFD, including area under the curve. *F*, fed insulin values at 16 weeks of HFD. *, $p < 0.05$; **, $p < 0.01$; $n = 5–8$ in WT→WT and TLR4$^{-/-}$ → *Tlr4*$^{-/-}$ and $n = 10–14$ in WT→*Tlr4*$^{-/-}$ and *Tlr4*$^{-/-}$→WT groups. (For fed insulin levels, $n = 2$ for WT→WT and $n = 4$ for *Tlr4*$^{-/-}$→*Tlr4*$^{-/-}$.) *Error bars*, S.E.

10 weeks of HFD, there were no differences in fasting glucose or fasting insulin levels (Fig. 2, *A* and *B*), but fasting free fatty acids (FFAs) were higher in WT→*Tlr4*$^{-/-}$ compared with *Tlr4*$^{-/-}$→WT animals (Fig. 2*C*). At 12 weeks of HFD, a glucose tolerance test demonstrated that *Tlr4*$^{-/-}$→WT animals had overall improved glucose tolerance (Fig. 2*E*), and after 16 weeks of HFD, even with similar fed glucose levels, insulin levels were lower in *Tlr4*$^{-/-}$ recipient animals (Fig. 2, *D* and *F*). These results suggest that both hematopoietic *Tlr4*$^{-/-}$ and whole-body *Tlr4*$^{-/-}$ contribute to the regulation of fatty acid and insulin levels, whereas glucose tolerance is related to hematopoietic TLR4 deficiency.

Leukocytes were evaluated in blood 2 weeks after BMT, and animals with WT BM had more B220^{+} cells in circulation, suggesting faster reconstitution (Fig. S2*A*). Two weeks after HFD exposure, there was a significant increase in circulating B220, Ly6G, and CD115^{+} myeloid cells in both WT recipient animals, but Ly6c^{hi} populations were similar (Fig. 3*A*). Adipose tissue evaluation at 16 weeks of HFD by flow cytometry (Fig. 3*B*) demonstrated equal CD45^{+} leukocytes and ATMs in GWAT (Fig. 3*D*) but a larger CD11c^{+}CD64^{+} ATM population in WT→*Tlr4*$^{-/-}$ compared with *Tlr4*$^{-/-}$→WT (Fig. 3*E*). Further quantification showed a significant increase in CD11c^{+} ATMs in GWAT of WT donor animals, whereas CD11c^{-} ATMs and dendritic cells (DCs) were equal in both groups (Fig. 3*F*). Gene expression showed a slight but nonsignificant decrease in *Tlr4* expression in *Tlr4*$^{-/-}$→WT GWAT (Fig. S2*B*) due to nonhematopoietic TLR4-expressing cells in adipose tissue.

To confirm appropriate reconstitution of these mice, hematopoietic progenitors and mature leukocytes were evaluated. CD3^{+} and CD4^{+} cells were decreased in BM of *Tlr4*$^{-/-}$→WT mice compared with WT→*Tlr4*$^{-/-}$ (Fig. S2*C*). Hematopoietic stem and progenitor cells were generally similar in both groups of reconstituted mice (Fig. S2*D*). Myeloid cells, however, were reduced in the spleen (CD11c^{+} and CD115^{+}) with an increase in CD19^{+} cells (Fig. S2*E*). In the blood, CD115^{+} and Ly6c^{hi} monocytes were also reduced, whereas circulating CD4^{+} cells were increased in mice with TLR4$^{-/-}$ BM (Fig. S2*F*). Both circulating and splenic monocyte profiles were consistent with a reduction in myeloid response to HFD in the absence of TLR4.

TLR4$^{-/-}$ *ATMs proliferate more robustly in response to HFD compared with WT ATMs*

Based on our findings of decreased recruited CD11c^{+} ATMs in animals with *Tlr4*$^{-/-}$ marrow, we anticipated that resident *Tlr4*$^{-/-}$ ATMs may expand earlier in HFD challenge, reducing the requirement for recruitment of myeloid cells to the adipose tissue. TLR4 activation in nonhematopoietic cells has been shown to inhibit cell proliferation (21, 22). To understand the initial macrophage response to adipose tissue expansion in TLR4 knockout animals, a short-term diet model was used wherein mice at 10 weeks of age were challenged with HFD until 12 weeks of age. After 2 weeks of HFD, body weights remained consistent with normal diet (ND)-fed animals in both WT and *Tlr4*$^{-/-}$ groups (Fig. 4*A*). GWAT pads expanded in both WT and *Tlr4*$^{-/-}$ animals (Fig. 4*B*), and GWAT immunofluorescence demonstrated more proliferating (Ki67^{+}) cells in the *Tlr4*$^{-/-}$ animals (Fig. 4*C*). Flow cytometry demonstrated that *Tlr4*$^{-/-}$ mice fed HFD had more ATMs (Fig. S3*A* and Fig. 4*D*). CD11c^{+} ATMs were increased in both WT and *Tlr4*$^{-/-}$ mice after 2 weeks of HFD, but only *Tlr4*$^{-/-}$ mice showed

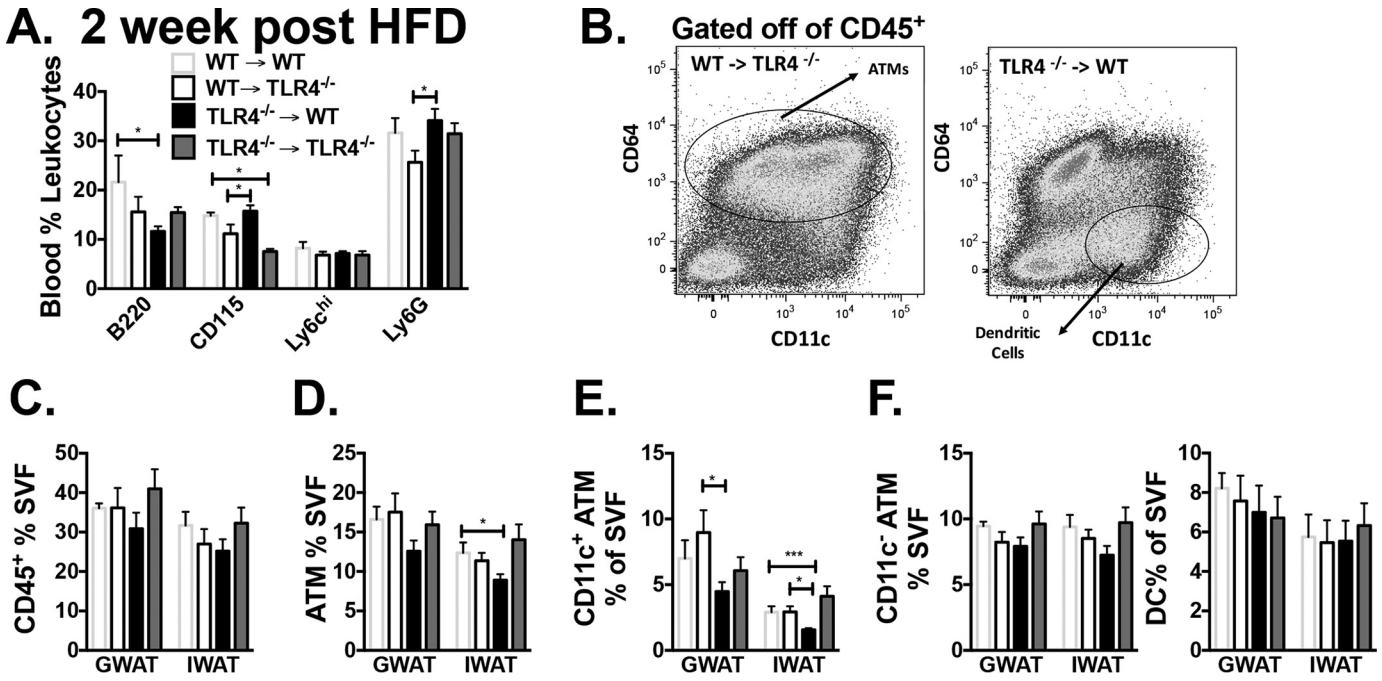

Figure 3. Decreased CD11c$^+$ ATMs in hematopoietic *Tlr4*$^{-/-}$ animals on high-fat diet. *A*, blood leukocytes were determined by flow cytometry 2 weeks after starting HFD. *B*, flow cytometry plot of CD45$^+$ cells in stromal vascular fraction. Shown is quantitation of CD45$^+$ cells in SVF (*C*), ATMs (*D*), CD11c$^+$ ATMs (*E*), and CD11c$^-$ ATMs, and dendritic cells (*DCs*) (*F*). *, $p < 0.05$; ***, $p < 0.005$; $n = 5$–7 in WT→WT and *Tlr4*$^{-/-}$→*Tlr4*$^{-/-}$ and $n = 11$–14 in WT→*Tlr4*$^{-/-}$ and *Tlr4*$^{-/-}$→WT groups. (For 2-week HFD blood monocytes, $n = 2$–4 in WT→WT, $n = 3$–7 in *Tlr4*$^{-/-}$→*Tlr4*$^{-/-}$, and $n = 6$–12 in WT→*Tlr4*$^{-/-}$ and *Tlr4*$^{-/-}$→WT groups.) *Error bars*, S.E.

expanded CD11c$^-$ ATMs (Fig. 4*D*). DCs were unchanged in either group. When we assessed proliferation, HFD caused proliferation of both ATM types; however, there was enhanced proliferation in CD11c$^-$ ATMs of *Tlr4*$^{-/-}$ animals compared with WT CD11c$^-$ ATMs (Fig. 4*E*). This increase in ATM proliferation was not seen after chronic HFD feeding in GWAT and IWAT, where a large number of both WT and *Tlr4*$^{-/-}$ leukocytes were proliferating compared with ND-fed animals (Fig. S3, *B* and *C*). We further challenged 10-week-old *Myd88*$^{-/-}$ and *Trif*$^{-/-}$ mice to 2 weeks of HFD and found that *Myd88*$^{-/-}$ mice mimic the results seen with the *Tlr4*$^{-/-}$ animals (Fig. 4*E*). These data demonstrate that TLR4 and MyD88 inhibit the ability of resident ATMs to proliferate with adipose tissue expansion in short-term HFD exposure.

Hematopoietic TRIF and MyD88 pathways contribute to myeloid expansion in obesity

We have previously shown that TLR4 and MyD88 pathways both regulate the generation of obesity-induced inflammation. Although TLR4 pathways were mostly necessary for long-term HSC expansion, MyD88 was mostly required for myeloid progenitor expansion, monocyte production, and hence ATM accumulation in obesity (2). Two competitive BMTs were designed to further define the role of MyD88, as well as to determine the role of the noncanonical TRIF (Ticam1) pathway in inflammation. First *Trif*$^{-/-}$ (CD45.2) and WT (CD45.1) BM was injected in a 1:1 ratio into irradiated CD45.1/CD45.2 heterozygous mice (Fig. 5*A*). These animals were started on HFD at 6 weeks post-BMT for 16 weeks. TRIF was required to expand pre-GMs, blood monocytes, and ATMs of both types, as seen from lower *Trif*$^{-/-}$ BM contribution to these cell types. To further delineate the role of MyD88 pathways, IRAKM, a negative regulator of MyD88 activation, was studied. *Irakm*$^{-/-}$ BM was competed with WT BM (Fig. 5*B*). *Irakm*$^{-/-}$ animal BM contributed to a greater number of pre-GMs, blood monocytes, and both types of ATMs, emphasizing a role for MyD88 pathways in generating bone marrow–derived myeloid cells during obesity (Fig. 5*B*). This same phenomenon for IRAKM pathways has been shown in LPS treatment of animals (23).

TLR4, TRIF, and MyD88 pathway knockouts respond with increased adiposity and glucose intolerance with HFD

WT, *Tlr4*$^{-/-}$, *Trif*$^{-/-}$, and *Myd88*$^{-/-}$ mice were placed on 60% HFD for 16 weeks. Animals in all groups gained weight (Fig. 6*A*), visceral fat (Fig. 6*B*), and subcutaneous fat (Fig. 6*C*) when challenged to HFD. Interestingly, liver mass did not increase in *Trif*$^{-/-}$ and was smaller overall in both *Trif*$^{-/-}$ and *Myd88*$^{-/-}$ mice with HFD compared with WT (Fig. 6*D*). Spleen weights were significantly larger after HFD in WT and *Trif*$^{-/-}$ mice (Fig. 6*E*). GWAT demonstrated increased adipocyte hypertrophy in all groups on HFD (Fig. 6*F*). Hematoxylin and eosin images of GWAT showed similar adipocyte hypertrophy but an increase in CLS and fibrosis in WT HFD-fed mice (Fig. 6*G*). Purely based on weight and adiposity, all groups were susceptible to obesity with HFD exposure.

Fasting glucose levels were not significantly different by genotype after 10 weeks on HFD but were lower in *Myd88*$^{-/-}$ mice on HFD compared with WT (Fig. 7*A*). Fasting insulin levels were substantially lower in all genotypes compared with WT (Fig. 7*B*). Glucose tolerance tests at 12 weeks on HFD were also unaffected by genotype (Fig. 7, *C* and *D*). Fed glucose levels were higher in mice on HFD, but insulin levels, although elevated in

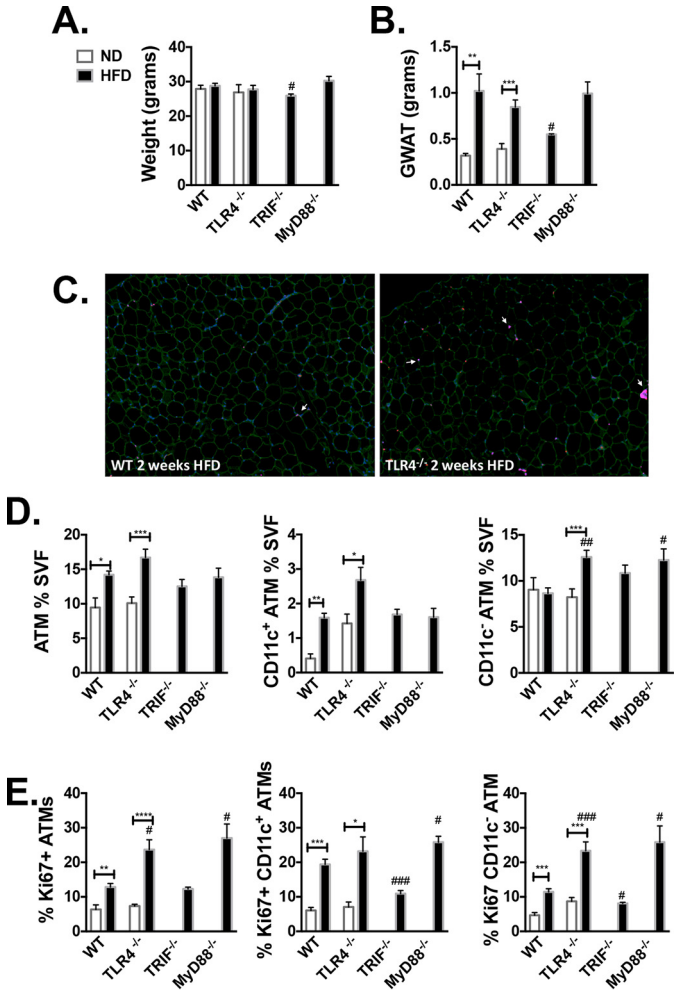

Figure 4. Increased CD11c$^-$ ATM proliferation in *Tlr4*$^{-/-}$ and *Myd88*$^{-/-}$ animals after short-term high-fat diet. 10-Week-old WT and TLR4$^{-/-}$ animals were challenged to ND or HFD for 2 weeks. At 12 weeks of age, weight (*A*) and GWAT (*B*) were assessed. *C*, immunostaining of GWAT with caveolin (*green*), Mac 2 (*magenta*), 4′,6-diamidino-2-phenylindole (*blue*), and Ki67 (*red*). *D*, ATM percentage of SVF, CD11c$^+$ ATM, and CD11c$^-$ ATM subsets as determined by flow cytometry. *E*, Ki67 proliferation as determined by intracellular flow cytometry staining in GWAT ATMs (CD11c$^+$ and CD11c$^-$ ATMs). *, $p < 0.05$; **, $p < 0.01$; ***, $p < 0.005$; ****, $p < 0.001$; ##, $p < 0.01$; ###, $p < 0.005$ between WT and knockout HFD ($n = 4$ WT ND, $n = 6$ *Tlr4*$^{-/-}$ ND, $n = 4$ WT HFD, $n = 10$ *Tlr4*$^{-/-}$ HFD, $n = 4$ *Trif*$^{-/-}$, and $n = 5$ *Myd88*$^{-/-}$ HFD). *Error bars*, S.E.

all groups, were lower in *Myd88*$^{-/-}$ animals (Fig. S4*A*). Fed FFAs were increased in WT and *Tlr4*$^{-/-}$ animals on HFD, whereas HFD-fed *Trif*$^{-/-}$ mice had lower FFAs in circulation (Fig. S4*B*) and lower liver TGs and decreased steatosis by histology (Fig. 4, *C* and *D*), consistent with the lack of increased liver weight (Fig. 6*D*).

TLR4, TRIF, and MyD88 pathways are required for generation of CD11c$^+$ ATMs

To next evaluate the adipose depot–specific inflammatory responses in the knockout models, ATMs were measured in both GWAT and IWAT by flow cytometry. WT, *Tlr4*$^{-/-}$, and *Myd88*$^{-/-}$ animals expanded total leukocytes and ATMs on HFD (Fig. 8, *A* and *B*), but *Trif*$^{-/-}$ animals preferentially increased DCs in IWAT with no change in ATMs or total leukocytes (Fig. 8*E*). Whereas WT, *Tlr4*$^{-/-}$, and *Myd88*$^{-/-}$ animals expanded CD11c$^+$ ATMs on HFD, CD11c$^+$ ATMs were significantly higher in WT HFD-fed animals when compared with *Tlr4*$^{-/-}$ and *Myd88*$^{-/-}$ HFD-fed animals ($p < 0.01$) (Fig. 8*C*). CD11c$^-$ ATM populations also expanded in obese *Tlr4*$^{-/-}$ and *Myd88*$^{-/-}$ mice similarly to WT mice; however, *Trif*$^{-/-}$ animals exhibited lower numbers of CD11c$^-$ ATMs (Fig. 8*D*). DCs were not significantly different in HFD-fed animals except for in the IWAT of *Tlr4*$^{-/-}$ and *Trif*$^{-/-}$ animals, and levels were increased in GWAT of *Myd88*$^{-/-}$ mice (Fig. 8*E*). This pattern of increased CD11c$^+$ ATMs in WT mice was supported by the appearance of more CLS in visceral adipose tissue by immunofluorescence in WT HFD-fed mice (Fig. 8*F*).

Gene expression analysis was examined in GWAT to confirm lack of *Tlr4*, *Ticam1* (*Trif*), and *Myd88* in the appropriate knockout animals (Fig. 8*G*). Evaluation of genes associated with adipose function showed increased *Tgfb* expression in GWAT with HFD, but no significant differences by genotype. *Glut4* and *Insr* expression levels were also reduced equally between genotypes (Fig. 8*G*), consistent with a decrease in insulin sensitivity. *Mcp1* was increased with HFD in WT, *Tlr4*$^{-/-}$, *Trif*$^{-/-}$, and *Myd88*$^{-/-}$ animals, although *Il1b* was highest in WT HFD-fed mice (Fig. 8*G*). Genes generally activated in CD11c$^-$ alternative resident macrophages, such as *Arg1* and *Tgfb*, showed increased expression in all groups. Hematopoietic compartment analysis demonstrated that granulocyte macrophage progenitors were only increased in WT animals on HFD (Fig. 8*H*), whereas pre-GMs were increased in all groups except the *Myd88*$^{-/-}$ HFD animals. Overall, these experiments demonstrate that the TLR4, TRIF, and MyD88 pathways are necessary for CD11c$^+$ ATM accumulation and myeloid progenitor expansion with HFD.

TLR4, MyD88, and TRIF are required for hematopoietic responses to saturated fatty acid

We employed *in vitro* myeloid colony-forming unit (cfu) assays to assess stem cell capacity in the obese knockout mice. Compared with WT HFD-fed controls, TLR4, TRIF, and MyD88 knockouts generated fewer myeloid colonies (Fig. 9*A*). To understand the mechanism of this effect, we stimulated BM with fatty acids or LPS *ex vivo* and then performed myeloid CFU assays. For these assays, we used saturated fatty acids (palmitic and stearic acid, 10 μM) and unsaturated fatty acids (linoleic and oleic acid, 10 μM). Whereas WT marrow increased cfu generation in response to saturated fatty acids, *Tlr4*$^{-/-}$, *Trif*$^{-/-}$, and *Myd88*$^{-/-}$ marrow did not respond with a similar increase in cfu (Fig. 9*B*). Similar results were seen with LPS treatment. Overall, oleic acid (an unsaturated fatty acid) decreased the saturated fatty acid response (Fig. 9*B*).

To determine whether this fatty acid response in myeloid cells was due to stimulation of mature cells or progenitors, we isolated lineage-negative (Lin$^-$) cells (immature noncommitted bone marrow cells), followed by treatment of isolated cells with palmitate. Palmitic acid stimulated WT lineage negative marrow (Fig. 9*C*), whereas *Tlr4*$^{-/-}$ lineage-negative BM was resistant to this stimulation and yielded lower colonies compared with WT lineage-negative PA treatment ($p = 0.06$).

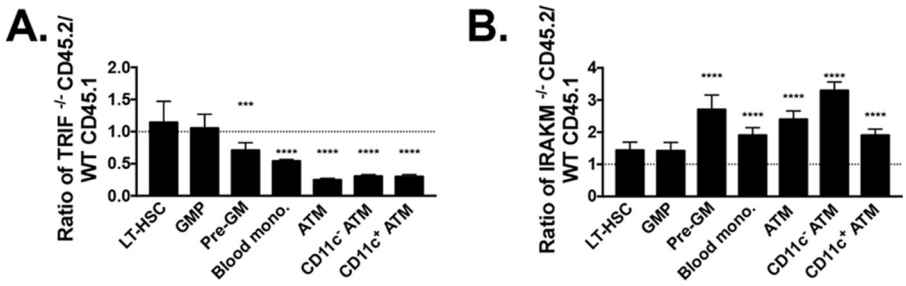

Figure 5. In competitive BMT models, TRIF and MyD88 pathways are necessary for expansion of myeloid progenitors and ATMs in response to HFD. Lethally irradiated CD45.1/CD45.2 heterozygote animals were injected with CD45.1 WT and CD45.2 *Trif*$^{-/-}$ BM in a 1:1 ratio (*A*) or CD45.1 WT and CD45.2 *Irakm*$^{-/-}$ BM in a 1:1 ratio (*B*). The ratio of quantitation of myeloid progenitors and leukocytes in animals reconstituted after 16 weeks of HFD (long-term hematopoietic stem cells (*LT-HSC*), granulocyte macrophage progenitor (*GMP*), pre-granulocyte macrophage (*Pre-GM*), blood monocytes, and ATMs and CD11c subsets) was calculated. ***, $p < 0.005$; ****, $p < 0.001$. $n = 9$ in TRIF competitive BMT and $n = 6$ in IRAKM competitive BMT. *Error bars*, S.E.

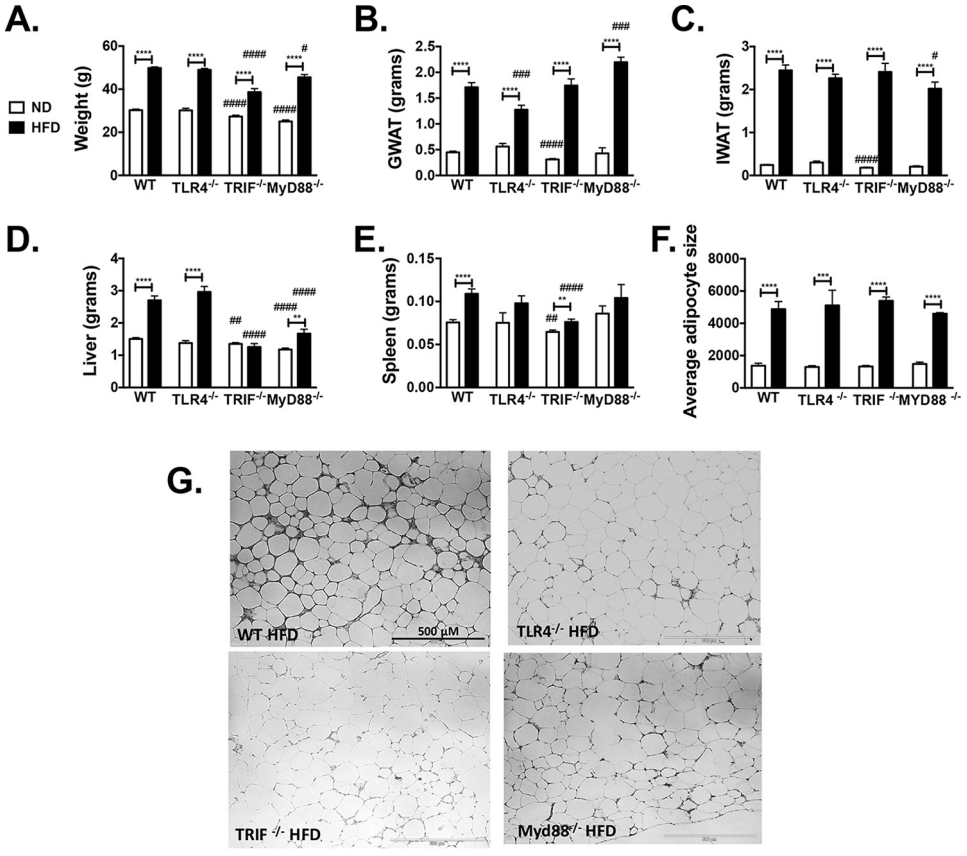

Figure 6. WT, *Tlr4*$^{-/-}$, *Trif*$^{-/-}$, and *MyD88*$^{-/-}$ animals respond to HFD challenge. Male animals were started on HFD at 6 weeks of age for 16 weeks. Shown are weight (*A*), GWAT weight (*B*), IWAT weight (*C*), liver weight (*D*), spleen weight (*E*), and average cross-sectional adipocyte size (*F*) of GWAT fat adipocytes. *G*, representative hematoxylin and eosin images of GWAT. **, $p < 0.01$; ***, $p < 0.005$; ****, $p < 0.001$. $n = 23$–24 in WT groups, $n = 14$–21 in *Tlr4*$^{-/-}$ groups, $n = 17$–19 in *Trif*$^{-/-}$, and $n = 5$–8 in *Myd88*$^{-/-}$ (for spleen weight, $n = 15$ ND and 16 HFD in WT groups, $n = 4$ ND and 10 HFD in *Tlr4*$^{-/-}$ groups, $n = 17$ ND and HFD in *Trif*$^{-/-}$, and $n = 5$ ND and 7 HFD for *Myd88*$^{-/-}$; for adipocyte sizing, $n = 8$–9 in WT groups, $n = 3$–4 in *Tlr4*$^{-/-}$ groups, and $n = 5$ in *Trif*$^{-/-}$ and *Myd88*$^{-/-}$). #, $p < 0.05$; ##, $p < 0.01$; ###, $p < 0.005$; ####, $p < 0.001$ when knockout groups were compared with WT ND or HFD control. *Error bars*, S.E.

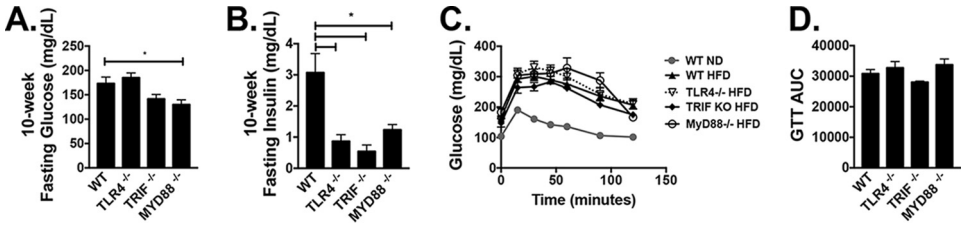

Figure 7. WT, *Tlr4*$^{-/-}$, *Trif*$^{-/-}$, and *Myd88*$^{-/-}$ animals respond metabolically to HFD challenge. Shown are 10-week fasting glucose ($n = 3$–8) (*A*) and insulin ($n = 3$–7) (*B*). Shown are 12-week glucose tolerance tests (WT ND, $n = 12$; WT HFD, $n = 21$; *Tlr4*$^{-/-}$ HFD, $n = 14$; *Trif*$^{-/-}$ HFD, $n = 4$; *Myd88*$^{-/-}$ HFD, $n = 6$) (*C*), with calculated area under curve (*AUC*) (*D*). *, $p < 0.05$. *Error bars*, S.E.

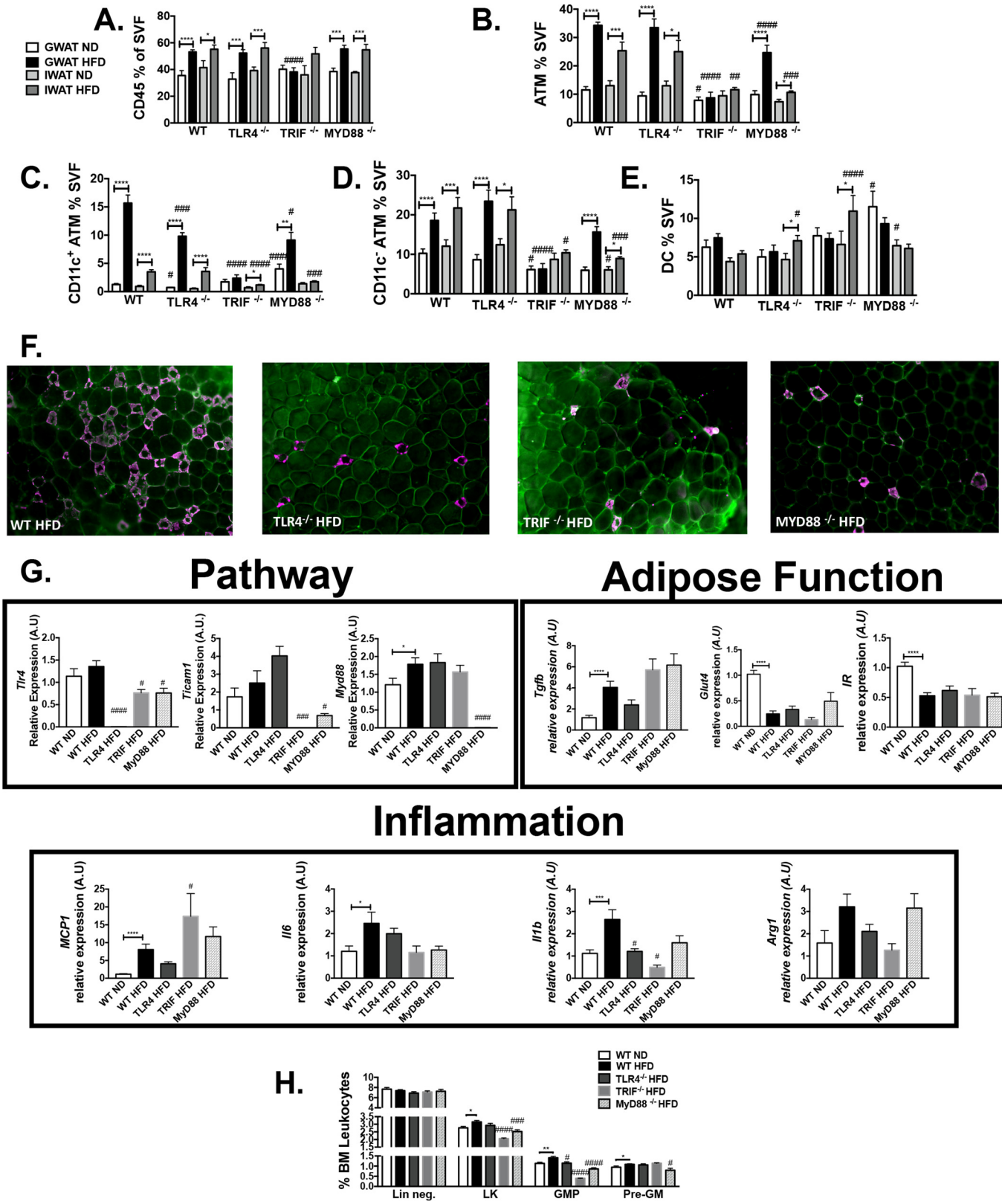

Figure 8. Tlr4$^{-/-}$, *Trif*$^{-/-}$, and *Myd88*$^{-/-}$ animals are protected from adipose tissue inflammation. After 16 weeks of HFD challenge, flow cytometry assessments were performed for CD45^{+} cells (*A*), ATMs (*B*), CD11c^{+} ATMs (*C*), CD11c^{-} ATMs (*D*), and DCs (*E*) (n = 12–21 in WT groups, n = 10–17 in *Tlr4*$^{-/-}$ groups, n = 7–17 in *Trif*$^{-/-}$, and n = 5–8 in *Myd88*$^{-/-}$). *F*, immunofluorescence in GWAT (caveolin (*green*) and Mac2 (*magenta*)). *G*, quantitative real-time PCR (n = 11 WT ND, n = 20 WT HFD, n = 10 *Tlr4*$^{-/-}$ HFD, n = 5 *Trif*$^{-/-}$ HFD, and n = 6 *MyD88*$^{-/-}$ HFD). *H*, flow cytometry evaluation of hematopoietic progenitors (n = 8 WT ND and HFD, n = 11 *Tlr4*$^{-/-}$, n = 5 *Trif*$^{-/-}$, and n = 8 *Myd88*$^{-/-}$). *, $p < 0.05$; **, $p < 0.01$; ***, $p < 0.005$; ****, $p < 0.001$; #, $p < 0.05$; ##, $p < 0.01$; ###, $p < 0.005$; ####, $p < 0.001$. *Error bars*, S.E.

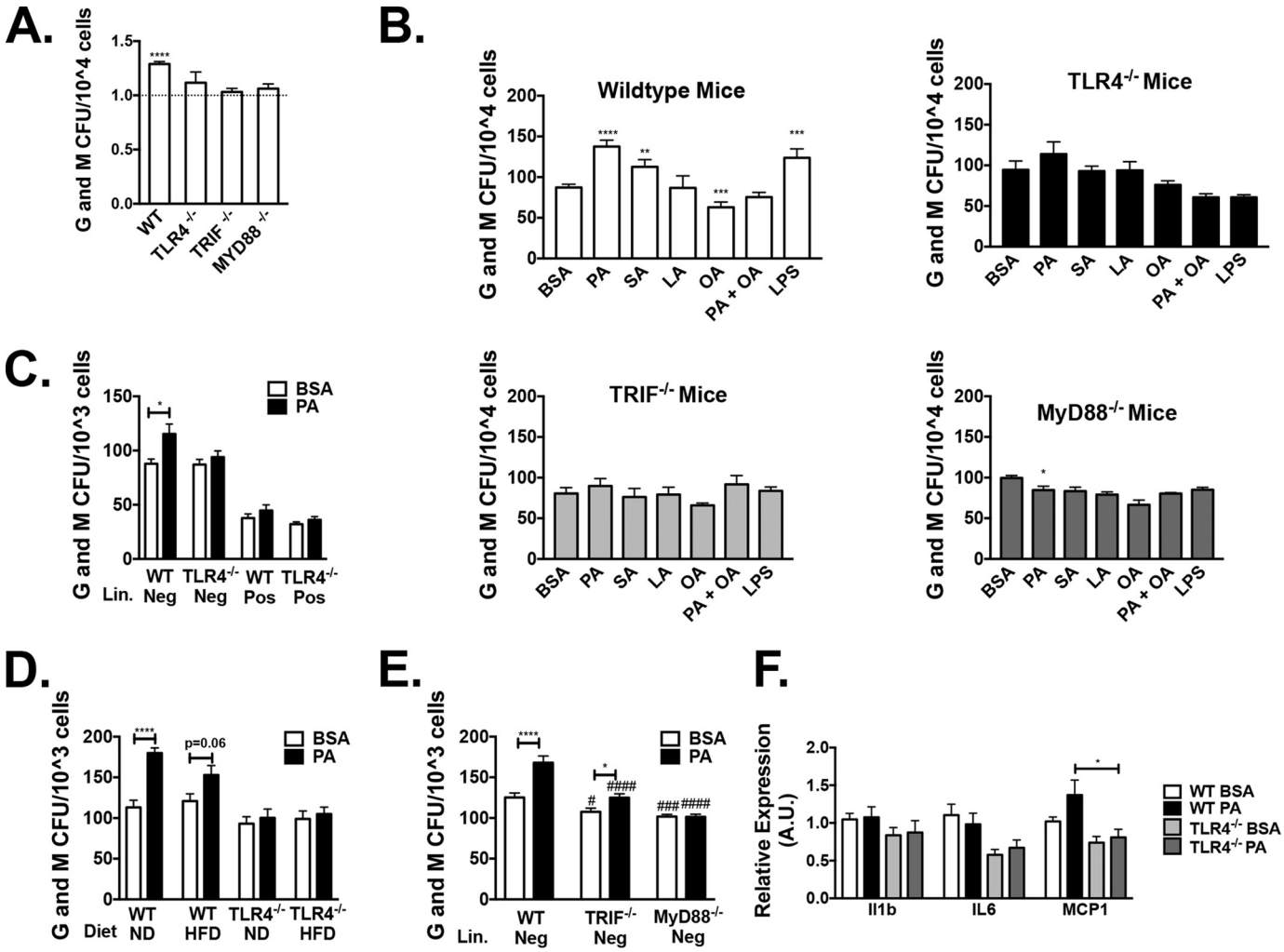

Figure 9. TLR4, MyD88, and TRIF are necessary for HFD and saturated fatty acid stimulation of myeloid colonies. After 16 weeks of ND or HFD, bone marrow was collected for myeloid methylcellulose colony-forming assays. *A*, ratio of HFD to ND myeloid colonies for WT, *Tlr4*$^{-/-}$, *Trif*$^{-/-}$, and *Myd88*$^{-/-}$ animals (n = 3–6). *B*, BM isolated from WT, *Tlr4*$^{-/-}$, *Trif*$^{-/-}$, and *Myd88*$^{-/-}$ animals were treated with fatty acid–free BSA or 10 μM fatty acid (PA, stearic acid (*SA*), linoleic acid (*LA*), oleic acid (*OA*), or LPS), and then colonies were counted after 7 days (n = 3 LPS and n = 6–15 for other groups). *C*, sorted lineage-negative or -positive cfu after BM treated with BSA or PA (n = 9 lineage-positive and n = 18 lineage-negative). *D*, myeloid colonies from lineage-negative ND and HFD-fed WT and *Tlr4*$^{-/-}$ animals (n = 6). *E*, lineage-negative marrow from WT, *Trif*$^{-/-}$, and *Myd88*$^{-/-}$ mice treated with BSA or PA (n = 9–14). *F*, gene expression from isolated colonies (n = 13). *, $p < 0.05$; **, $p < 0.01$; ***, $p < 0.005$; ****, $p < 0.001$ compared with control. #, $p < 0.05$; ###, $p < 0.005$; ####, $p < 0.001$ when knockout groups were compared with WT. *Error bars*, S.E.

Comparison of WT and *Tlr4*$^{-/-}$ ND and HFD animals showed a brisk response to PA in ND WT mice that was blunted in HFD WT mice. *Tlr4*$^{-/-}$ mice on ND or HFD failed to induce colony formation in response to PA in Lin$^-$ cells (Fig. 9*D*). Lin$^-$ TRIF and MyD88 knockout mice demonstrated that *Myd88*$^-$, but not *Trif*, was required for myeloid expansion in response to PA (Fig. 9*E*); however, both pathways yielded lower myeloid colonies compared with WT mice. This was consistent with our prior research (2) that determined that MyD88 pathways are critical for myeloid inflammation in obesity. Gene expression studies in harvested cells treated with PA (Fig. 9*F*) demonstrated that palmitate stimulation in WT mice, but not *Tlr4*$^{-/-}$ animals, induced *Mcp1* expression (analysis of variance, $p <$ 0.05).

Discussion

Our findings show that there are distinct roles for TLR4, TRIF, and MyD88 in the inflammatory response to obesity. Prior studies have identified a role for TLR4 and NF-κB (24) in obesity-induced inflammation and insulin resistance (25). Our studies demonstrate that TLR4 reduces local (CD11c$^-$) macrophage proliferation in response to adipose tissue expansion, promotes recruitment of CD11c$^+$ ATM accumulation, and is also necessary for the generation of bone marrow–derived macrophages in response to saturated fatty acid.

Spontaneous mutants lacking TLR4 function are protected from insulin resistance (26), but studies have shown mixed effects of TLR4 knockouts in the metabolic response to HFD. Our reciprocal BMTs suggest that this may be because of opposing TLR4 function in bone marrow–derived and nonhematopoietic compartments, such as adipocytes. Whereas animals reconstituted with *Tlr4*$^{-/-}$ BM had improved metabolism, glucose tolerance in nonirradiated *Tlr4*$^{-/-}$ mice on HFD showed similar impairment as WT HFD-fed animals (Fig. 7). *Tlr4*$^{-/-}$ mice gained significantly more weight when nonirradiated, suggesting that the protection conferred by hematopoi-

etic TLR4 deficiency may be overcome by excess adiposity. TLR4 has a known role in adipocytes (27), especially in short-term HFD, and in recruitment of inflammatory leukocytes (28). Once chronic obesity has led to expansion of adipose tissue, there is probably a secondary role for TLR4 in the generation of fibrosis, promoting further adipose tissue dysfunction (20).

TLR4 and MyD88 have specifically been reported to be critical for ATMs that are "metabolically activated" and play an important role in adipose tissue homeostasis (30). Our results suggest that MyD88 deficiency protects from meta-inflammation because MyD88 is required for accumulation of activated ATMs and enhanced myelopoiesis. Our results are consistent with previous studies (31, 32) that have implicated MyD88 in its contribution to obesity-induced adipose tissue inflammation (31), atherosclerosis (31, 33), and improved glucose sensitivity (34). Studies have previously demonstrated that MyD88 is necessary for TLR2 and TLR4 saturated fatty acid–induced inflammatory activation of mature macrophages (35). Additionally, our results demonstrate that MyD88 pathways are also responsible for the HSC responses to saturated fatty acids in obesity.

Whereas MyD88-independent TRIF signaling has been implicated in hematopoiesis (36) and atherosclerosis (37), there is a paucity of data on the role of TRIF in meta-inflammation. We found that Lin^- $Trif^{-/-}$ progenitors produced myeloid colonies in response to palmitate stimulation *in vitro*. *In vivo*, however, $Trif^{-/-}$ animals had fewer myeloid progenitors and ATMs with HFD challenge when compared with WT animals. It is interesting to note that although these animals gained weight and adiposity, $Trif^{-/-}$ mice were protected from hepatic steatosis and triglyceride accumulation during HFD. This finding is contrary to what has been observed in models of nonalcoholic steatohepatitis, where $Trif^{-/-}$ animals generally have increased inflammation and fibrosis due to enhanced stellate cell chemokine and cytokine activation of the MyD88 pathway, demonstrating that TRIF is probably important for inhibiting inflammation in the liver (38, 39). However, inflammation is provoked in those studies through amino acid deficiency as opposed to HFD-induced obesity stimulation. This highlights the importance of source and degree of stimulation when evaluating steatosis and hepatic inflammation (40, 41). This also emphasizes that there may be a potential different role for TRIF pathways in the adipose tissue protecting HFD-fed $Trif^{-/-}$ mice from adipose tissue inflammation and dysfunction, leading to protection from fatty acid release and steatosis.

The role of TLR4 pathways in biasing hematopoietic progenitor expansion (42) toward myelopoiesis (43) with LPS stimulation has been demonstrated in acute settings but remains unresolved in the chronic inflammatory state of obesity. The studies here reveal that TLR4 through TRIF and MyD88 signaling cascades are important for hematopoietic contribution to myeloid cells and macrophage polarization in obesity-induced inflammation. The importance of TLR4 in bone marrow–derived myeloid cells for insulin resistance during obesity has only recently been characterized (2, 44, 45), but with a limited understanding of its triggers. Our BM studies indicate that saturated fatty acids have a direct role in enhancing myeloid progenitors via stimulation of TLR4, TRIF, and MyD88 pathways.

Whereas this direct effect of fatty acids on hematopoietic progenitors is novel, it is probably one of many factors altered with HFD, given that increased endotoxins (46) and microbiota changes have also been demonstrated to enhance ATM recruitment via TLR4 (47).

Another limitation of our studies is that the TRIF and MyD88 knockout animal results are possibly confounded by signaling pathways from other TLRs that are activated during an obese state, including TLR2 (48, 49). Also, it is not clear whether this increased TLR4 activation in hematopoietic progenitors through TRIF pathways leads to tolerance or exhaustion in chronic HFD, as has been demonstrated in LPS stimulation (36, 50). Timing and dose of stimulation are critical in LPS studies (51) and hence may not mimic findings in obesity. Further, whereas we were able to characterize the role of TLR4 via MyD88 for inhibition of local $CD11c^-$ ATM proliferation and the role of both TRIF and MyD88 for myeloid progenitor expansion, the downstream pathways from this initial signaling are yet to be determined.

Overall, our studies demonstrate that TLR4, TRIF, and MyD88 play critical roles in the profile of ATMs in visceral fat after acute and chronic HFD exposure. In addition, deficiency of any of these pathways reduces myeloid stimulation of bone marrow with saturated fatty acids. These results emphasize that when evaluating obesity-induced inflammation, the tissue-specific macrophage response may only be part of the underlying effect and that there is an additional myeloid progenitor alteration that occurs with obesity.

Experimental procedures

Animal models and treatments

C57Bl/6J (WT), $Tlr4^{-/-}$ (B6.B10ScN-$Tlr4^{lps\text{-}del}$/JthJ; 007227), and $Myd88^{-/-}$ (B6.129P2 (SJL)-$Myd88^{tm.1.1Defr}$/J; 009088) mice on C57Bl/6J background were purchased from Jackson Laboratories. $Trif^{-/-}$ mice were donated from Dr. Gabriel Nunez's laboratory, originally from the Akira laboratory (52). $Irakm^{-/-}$ mice were donated from a colony bred on a B6 background that was established at the University of Michigan (53). All mice were male and were fed *ad libitum* either a control ND consisting of 4.5% fat (5001; LabDiet) or an HFD consisting of 60% of calories from fat (Research Diets, Inc., D12492) starting at 6 weeks of age for 16 weeks duration. Glucose tolerance (with 0.7 g/kg) and insulin tolerance (with 1 unit/kg) testing were performed after 6 h of fasting. Animals were housed in a specific pathogen-free facility with a 12-h light/12-h dark cycle and given free access to food and water. Animal protocols were in compliance with the Institute of Laboratory Animal Research Guide for the Care and Use of Laboratory Animals and approved by the University Committee on Use and Care of Animals at the University of Michigan (animal welfare assurance number A3114-01).

Quantitative real-time PCR

RNA extraction was performed with an RNeasy kit (Qiagen) followed by reverse transcription (Applied Biosystems) and real-time PCR analysis using glyceraldehyde-3-phosphate dehydrogenase to normalize (SYBR Green, ABI Prism 7200 Sequence Detection System; Applied Biosystems). Relative

Table 1
Primer sequences

	Forward primer	Reverse primer
Gapdh	TGAAGCAGGCATCTGAGGG	CGAAGGTGGAAGAGTGGGAG
Il6	TAGTCCTTCCTACCCCAATTTCC	AAGGAACCCTTAGAGTGCTTACT
Mcp1	TTAAAAACCTGGATCGGAACCAA	GCATTAGCTTCAGATTTACGGGT
Il1b	AAATACCTGTGGCCTTGGGC	CTTGGGATCCACACTCTCCAG
Arg1	CTCCAAGCCAAAGTCCTTAGAG	AGGAGCTGTCATTAGGGACATC
Tgfb	GGACTCTCCACCTGCAAGAC	GACTGGCGAGCCTTAGTTTG
Tlr4	ATGGCATGGCTTACACCACC	GAGGCCAATTTTGTCTCCACA
Ticam1	CCAGCTCAAGACCCCTACAG	CAAGGCACCTAGAATGCCAAA
Myd88	AGGACAAACGCCGGAACTTTT	GCCGATAGTCTGTCTGTTCTAGT
Ir	TTTGTCATGGATGGAGGCTA	CCTCATCTTGGGGTTGAACT
Glut4	GTGACTGGAACACTGGTCCTA	CCAGCCACGTTGCATTGTAG

expression was assessed by the comparative *CT* method correcting for amplification efficiency of the primers and performed in duplicate as described previously (2). PCR primers used are reported in Table 1.

Adipose tissue stromal vascular fraction (SVF) isolation and flow cytometry

Adipose tissue fractionation and flow cytometry analyses were performed as described previously after Fc blocking of samples (54). SVF cells were stained with CD64 PE, CD45.2 e450, and CD11c-APC-Cy7 or APC (eBioscience) (55) for ATMs.

Flow cytometry assessment of HSC and myeloid progenitors

Bone marrow from one femur was flushed with PBS and made into single-cell suspension using a syringe and then centrifuged. Thereafter, cell pellets were treated with RBC lysis solution for 5 min. After resuspension in PBS, cells were stained with lineage markers on APC (CD4, CD5, CD8, CD11b, B220 (CD45R), Gr1, Ter119), CD117-APC-Cy7, Sca1-PECy7, CD16/32 PerCP5.5 (eBioscience), CD150-PE, Endoglin-Pacific Blue (Biolegend), CD48 FITC, and gating as described by Pronk *et al.* (56) and Oguro *et al.* (57).

cfu assays

Bone marrow from a femur was flushed with Iscove's modified Dulbecco's medium. This marrow was then treated with fatty acid–free BSA, with fatty acids (palmitic acid, linoleic acid, oleic acid, stearic acid) (10 μM, purchased from Sigma) in fatty acid–free BSA, or with 10 μg/ml LPS for 1 h at 37 °C. Cells were then resuspended in MethoCult medium and plated at a density of 10,000 cells/plate/protocol (Stem Cell Technology). After 7 days, colonies were counted. For sorted cfu assays, bone marrow was isolated from animals, and lineage-negative cells were separated using a stem-cell magnet column isolation kit (EasySep™ hematopoietic progenitor cell enrichment kit). After magnetic separation, 1000 cells were used per plate.

Bone marrow transplantation

Bone marrow cells were isolated from donor groups (58) and injected retro-orbitally into lethally irradiated (900 rads) 6-week-old recipient mice (10 million cells/mouse). Animals were treated with antibiotics (polymyxin and neomycin) for 4 weeks after BMT. Following 2 weeks of normal chow diet, they were started on ND or HFD chow. Glucose tolerance testing was performed as described previously (29).

Statistics

Results are presented as mean ± S.E. One-way or two-way analysis of variance was performed with factors of genotype and diet. If there was a main effect for either factor, then *t* tests were performed for WT *versus* knockout differences within each diet or for diet groups within each group, respectively.

Author contributions—C. G., L. E., N. L., S. A., M. V., K. M., L. M., J. L., and K. S. data curation; C. G., L. E., N. L., S. A., K. M., J. L., and K. S. formal analysis; C. G., S. A., and K. S. supervision; C. G. and K. S. methodology; C. G., S. A., and K. S. writing-original draft; L. E., N. L., M. V., C. N. L., and K. S. writing-review and editing; S. A. and K. S. investigation; L. M., C. N. L., and K. S. conceptualization; C. N. L. resources; C. N. L. and K. S. funding acquisition; K. S. validation; K. S. visualization; K. S. project administration.

Acknowledgments—We thank Nidhi Maley, Dr. Brian Zamarron, Dr. Gabriel Martinez-Santibanez, Dr. Eric Chang, and Devyani Agarwal for assistance during experiments. This work utilized Core Services from the Michigan Nutrition and Obesity Research Center supported by National Institutes of Health Grant DK089503 to the University of Michigan.

References

1. Saltiel, A. R., and Olefsky, J. M. (2017) Inflammatory mechanisms linking obesity and metabolic disease. *J. Clin. Invest.* **127,** 1–4 CrossRef Medline
2. Singer, K., DelProposto, J., Morris, D. L., Zamarron, B., Mergian, T., Maley, N., Cho, K. W., Geletka, L., Subbaiah, P., Muir, L., Martinez-Santibanez, G., and Lumeng, C. N. (2014) Diet-induced obesity promotes myelopoiesis in hematopoietic stem cells. *Mol. Metab.* **3,** 664–675 CrossRef Medline
3. Amano, S. U., Cohen, J. L., Vangala, P., Tencerova, M., Nicoloro, S. M., Yawe, J. C., Shen, Y., Czech, M. P., and Aouadi, M. (2014) Local proliferation of macrophages contributes to obesity-associated adipose tissue inflammation. *Cell Metab.* **19,** 162–171 CrossRef Medline
4. Lumeng, C. N., Bodzin, J. L., and Saltiel, A. R. (2007) Obesity induces a phenotypic switch in adipose tissue macrophage polarization. *J. Clin. Invest.* **117,** 175–184 CrossRef Medline
5. Crewe, C., An, Y. A., and Scherer, P. E. (2017) The ominous triad of adipose tissue dysfunction: inflammation, fibrosis, and impaired angiogenesis. *J. Clin. Invest.* **127,** 74–82 CrossRef Medline
6. Carvalheira, J. B., Qiu, Y., and Chawla, A. (2013) Blood spotlight on leukocytes and obesity. *Blood* **122,** 3263–3267 CrossRef Medline
7. Wentworth, J. M., Naselli, G., Brown, W. A., Doyle, L., Phipson, B., Smyth, G. K., Wabitsch, M., O'Brien, P. E., and Harrison, L. C. (2010) Pro-inflammatory $CD11c^+CD206^+$ adipose tissue macrophages are associated with insulin resistance in human obesity. *Diabetes* **59,** 1648–1656 CrossRef Medline

8. Sartipy, P., and Loskutoff, D. J. (2003) Monocyte chemoattractant protein 1 in obesity and insulin resistance. *Proc. Natl. Acad. Sci. U.S.A.* **100,** 7265–7270 CrossRef Medline
9. Cho, K. W., Zamarron, B. F., Muir, L. A., Singer, K., Porsche, C. E., DelProposto, J. B., Geletka, L., Meyer, K. A., O'Rourke, R. W., and Lumeng, C. N. (2016) Adipose tissue dendritic cells are independent contributors to obesity-induced inflammation and insulin resistance. *J. Immunol.* **197,** 3650–3661 CrossRef Medline
10. Xu, X., Grijalva, A., Skowronski, A., van Eijk, M., Serlie, M. J., and Ferrante, A. W., Jr. (2013) Obesity activates a program of lysosomal-dependent lipid metabolism in adipose tissue macrophages independently of classic activation. *Cell Metab.* **18,** 816–830 CrossRef Medline
11. Kratz, M., Coats, B. R., Hisert, K. B., Hagman, D., Mutskov, V., Peris, E., Schoenfelt, K. Q., Kuzma, J. N., Larson, I., Billing, P. S., Landerholm, R. W., Crouthamel, M., Gozal, D., Hwang, S., Singh, P. K., and Becker, L. (2014) Metabolic dysfunction drives a mechanistically distinct proinflammatory phenotype in adipose tissue macrophages. *Cell Metab.* **20,** 614–625 CrossRef Medline
12. Li, P., Lu, M., Nguyen, M. T., Bae, E. J., Chapman, J., Feng, D., Hawkins, M., Pessin, J. E., Sears, D. D., Nguyen, A. K., Amidi, A., Watkins, S. M., Nguyen, U., and Olefsky, J. M. (2010) Functional heterogeneity of CD11c-positive adipose tissue macrophages in diet-induced obese mice. *J. Biol. Chem.* **285,** 15333–15345 CrossRef Medline
13. Singer, K., Maley, N., Mergian, T., DelProposto, J., Cho, K. W., Zamarron, B. F., Martinez-Santibanez, G., Geletka, L., Muir, L., Wachowiak, P., Demirjian, C., and Lumeng, C. N. (2015) Differences in hematopoietic stem cells contribute to sexually dimorphic inflammatory responses to high fat diet-induced obesity. *J. Biol. Chem.* **290,** 13250–13262 CrossRef Medline
14. Lawrence, T. (2009) The nuclear factor NF-κB pathway in inflammation. *Cold Spring Harb. Perspect. Biol.* **1,** a001651 Medline
15. Rossol, M., Heine, H., Meusch, U., Quandt, D., Klein, C., Sweet, M. J., and Hauschildt, S. (2011) LPS-induced cytokine production in human monocytes and macrophages. *Crit. Rev. Immunol.* **31,** 379–446 CrossRef Medline
16. Akira, S., and Takeda, K. (2004) Toll-like receptor signalling. *Nat. Rev. Immunol.* **4,** 499–511 CrossRef Medline
17. Shi, H., Kokoeva, M. V., Inouye, K., Tzameli, I., Yin, H., and Flier, J. S. (2006) TLR4 links innate immunity and fatty acid-induced insulin resistance. *J. Clin. Invest.* **116,** 3015–3025 CrossRef Medline
18. Saberi, M., Woods, N. B., de Luca, C., Schenk, S., Lu, J. C., Bandyopadhyay, G., Verma, I. M., and Olefsky, J. M. (2009) Hematopoietic cell-specific deletion of toll-like receptor 4 ameliorates hepatic and adipose tissue insulin resistance in high-fat-fed mice. *Cell Metab.* **10,** 419–429 CrossRef Medline
19. Orr, J. S., Puglisi, M. J., Ellacott, K. L., Lumeng, C. N., Wasserman, D. H., and Hasty, A. H. (2012) Toll-like receptor 4 deficiency promotes the alternative activation of adipose tissue macrophages. *Diabetes* **61,** 2718–2727 CrossRef Medline
20. Vila, I. K., Badin, P. M., Marques, M. A., Monbrun, L., Lefort, C., Mir, L., Louche, K., Bourlier, V., Roussel, B., Gui, P., Grober, J., Štich, V., Rossmeislová, L., Zakaroff-Girard, A., Bouloumié, A., *et al.* (2014) Immune cell Toll-like receptor 4 mediates the development of obesity- and endotoxemia-associated adipose tissue fibrosis. *Cell Rep.* **7,** 1116–1129 CrossRef Medline
21. Wang, Y., Abarbanell, A. M., Herrmann, J. L., Weil, B. R., Manukyan, M. C., Poynter, J. A., and Meldrum, D. R. (2010) TLR4 inhibits mesenchymal stem cell (MSC) STAT3 activation and thereby exerts deleterious effects on MSC-mediated cardioprotection. *PLoS One* **5,** e14206 CrossRef Medline
22. Sodhi, C. P., Shi, X. H., Richardson, W. M., Grant, Z. S., Shapiro, R. A., Prindle, T., Jr., Branca, M., Russo, A., Gribar, S. C., Ma, C., and Hackam, D. J. (2010) Toll-like receptor-4 inhibits enterocyte proliferation via impaired β-catenin signaling in necrotizing enterocolitis. *Gastroenterology* **138,** 185–196 CrossRef Medline
23. Kobayashi, K., Hernandez, L. D., Galán, J. E., Janeway, C. A., Jr., Medzhitov, R., and Flavell, R. A. (2002) IRAK-M is a negative regulator of Toll-like receptor signaling. *Cell* **110,** 191–202 CrossRef Medline
24. Gregor, M. F., and Hotamisligil, G. S. (2011) Inflammatory mechanisms in obesity. *Annu. Rev. Immunol.* **29,** 415–445 CrossRef Medline
25. Deng, Z. B., Poliakov, A., Hardy, R. W., Clements, R., Liu, C., Liu, Y., Wang, J., Xiang, X., Zhang, S., Zhuang, X., Shah, S. V., Sun, D., Michalek, S., Grizzle, W. E., Garvey, T., Mobley, J., and Zhang, H. G. (2009) Adipose tissue exosome-like vesicles mediate activation of macrophage-induced insulin resistance. *Diabetes* **58,** 2498–2505 CrossRef Medline
26. Poggi, M., Bastelica, D., Gual, P., Iglesias, M. A., Gremeaux, T., Knauf, C., Peiretti, F., Verdier, M., Juhan-Vague, I., Tanti, J. F., Burcelin, R., and Alessi, M. C. (2007) C3H/HeJ mice carrying a toll-like receptor 4 mutation are protected against the development of insulin resistance in white adipose tissue in response to a high-fat diet. *Diabetologia* **50,** 1267–1276 CrossRef Medline
27. Norseen, J., Hosooka, T., Hammarstedt, A., Yore, M. M., Kant, S., Aryal, P., Kiernan, U. A., Phillips, D. A., Maruyama, H., Kraus, B. J., Usheva, A., Davis, R. J., Smith, U., and Kahn, B. B. (2012) Retinol-binding protein 4 inhibits insulin signaling in adipocytes by inducing proinflammatory cytokines in macrophages through a c-Jun N-terminal kinase- and toll-like receptor 4-dependent and retinol-independent mechanism. *Mol. Cell. Biol.* **32,** 2010–2019 CrossRef Medline
28. Tao, C., Holland, W. L., Wang, Q. A., Shao, M., Jia, L., Sun, K., Lin, X., Kuo, Y. C., Johnson, J. A., Gordillo, R., Elmquist, J. K., and Scherer, P. E. (2017) Short-term *versus* long-term effects of adipocyte Toll-like receptor 4 activation on insulin resistance in male mice. *Endocrinology* **158,** 1260–1270 CrossRef Medline
29. Westcott, D. J., Delproposto, J. B., Geletka, L. M., Wang, T., Singer, K., Saltiel, A. R., and Lumeng, C. N. (2009) MGL1 promotes adipose tissue inflammation and insulin resistance by regulating 7/4hi monocytes in obesity. *J. Exp. Med.* **206,** 3143–3156 CrossRef Medline
30. Coats, B. R., Schoenfelt, K. Q., Barbosa-Lorenzi, V. C., Peris, E., Cui, C., Hoffman, A., Zhou, G., Fernandez, S., Zhai, L., Hall, B. A., Haka, A. S., Shah, A. M., Reardon, C. A., Brady, M. J., Rhodes, C. J., *et al.* (2017) Metabolically activated adipose tissue macrophages perform detrimental and beneficial functions during diet-induced obesity. *Cell Rep.* **20,** 3149–3161 CrossRef Medline
31. Yu, M., Zhou, H., Zhao, J., Xiao, N., Roychowdhury, S., Schmitt, D., Hu, B., Ransohoff, R. M., Harding, C. V., Hise, A. G., Hazen, S. L., DeFranco, A. L., Fox, P. L., Morton, R. E., Dicorleto, P. E., *et al.* (2014) MyD88-dependent interplay between myeloid and endothelial cells in the initiation and progression of obesity-associated inflammatory diseases. *J. Exp. Med.* **211,** 887–907 CrossRef Medline
32. Nagareddy, P. R., Kraakman, M., Masters, S. L., Stirzaker, R. A., Gorman, D. J., Grant, R. W., Dragoljevic, D., Hong, E. S., Abdel-Latif, A., Smyth, S. S., Choi, S. H., Korner, J., Bornfeldt, K. E., Fisher, E. A., Dixit, V. D., *et al.* (2014) Adipose tissue macrophages promote myelopoiesis and monocytosis in obesity. *Cell Metab.* **19,** 821–835 CrossRef Medline
33. Kleinridders, A., Schenten, D., Könner, A. C., Belgardt, B. F., Mauer, J., Okamura, T., Wunderlich, F. T., Medzhitov, R., and Brüning, J. C. (2009) MyD88 signaling in the CNS is required for development of fatty acid-induced leptin resistance and diet-induced obesity. *Cell Metab.* **10,** 249–259 CrossRef Medline
34. Hosoi, T., Yokoyama, S., Matsuo, S., Akira, S., and Ozawa, K. (2010) Myeloid differentiation factor 88 (MyD88)-deficiency increases risk of diabetes in mice. *PLoS One* **5,** e12537 CrossRef Medline
35. Huang, S., Rutkowsky, J. M., Snodgrass, R. G., Ono-Moore, K. D., Schneider, D. A., Newman, J. W., Adams, S. H., and Hwang, D. H. (2012) Saturated fatty acids activate TLR-mediated proinflammatory signaling pathways. *J. Lipid Res.* **53,** 2002–2013 CrossRef Medline
36. Takizawa, H., Fritsch, K., Kovtonyuk, L. V., Saito, Y., Yakkala, C., Jacobs, K., Ahuja, A. K., Lopes, M., Hausmann, A., Hardt, W. D., Gomariz, Á., Nombela-Arrieta, C., and Manz, M. G. (2017) Pathogen-induced TLR4-TRIF innate immune signaling in hematopoietic stem cells promotes proliferation but reduces competitive fitness. *Cell Stem Cell* **21,** 225–240.e5 CrossRef Medline
37. Richards, M. R., Black, A. S., Bonnet, D. J., Barish, G. D., Woo, C. W., Tabas, I., Curtiss, L. K., and Tobias, P. S. (2013) The LPS2 mutation in TRIF is atheroprotective in hyperlipidemic low density lipoprotein receptor knockout mice. *Innate Immun.* **19,** 20–29 CrossRef Medline

38. Yang, L., Miura, K., Zhang, B., Matsushita, H., Yang, Y. M., Liang, S., Song, J., Roh, Y. S., and Seki, E. (2017) TRIF differentially regulates hepatic steatosis and inflammation/fibrosis in mice. *Cell Mol. Gastroenterol. Hepatol.* **3,** 469–483 CrossRef Medline
39. Chen, J., Li, J., Yiu, J. H. C., Lam, J. K. W., Wong, C. M., Dorweiler, B., Xu, A., and Woo, C. W. (2017) TRIF-dependent Toll-like receptor signaling suppresses Scd1 transcription in hepatocytes and prevents diet-induced hepatic steatosis. *Sci. Signal.* **10,** eaal3336 CrossRef Medline
40. Deng, Z. B., Liu, Y., Liu, C., Xiang, X., Wang, J., Cheng, Z., Shah, S. V., Zhang, S., Zhang, L., Zhuang, X., Michalek, S., Grizzle, W. E., and Zhang, H. G. (2009) Immature myeloid cells induced by a high-fat diet contribute to liver inflammation. *Hepatology* **50,** 1412–1420 CrossRef Medline
41. Li, L., Chen, L., Hu, L., Liu, Y., Sun, H. Y., Tang, J., Hou, Y. J., Chang, Y. X., Tu, Q. Q., Feng, G. S., Shen, F., Wu, M. C., and Wang, H. Y. (2011) Nuclear factor high-mobility group box1 mediating the activation of Toll-like receptor 4 signaling in hepatocytes in the early stage of nonalcoholic fatty liver disease in mice. *Hepatology* **54,** 1620–1630 CrossRef Medline
42. Liu, A., Wang, Y., Ding, Y., Baez, I., Payne, K. J., and Borghesi, L. (2015) Cutting edge: hematopoietic stem cell expansion and common lymphoid progenitor depletion require hematopoietic-derived, cell-autonomous TLR4 in a model of chronic endotoxin. *J. Immunol.* **195,** 2524–2528 CrossRef Medline
43. Boettcher, S., Ziegler, P., Schmid, M. A., Takizawa, H., van Rooijen, N., Kopf, M., Heikenwalder, M., and Manz, M. G. (2012) Cutting edge: LPS-induced emergency myelopoiesis depends on TLR4-expressing nonhematopoietic cells. *J. Immunol.* **188,** 5824–5828 CrossRef Medline
44. Razolli, D. S., Moraes, J. C., Morari, J., Moura, R. F., Vinolo, M. A., and Velloso, L. A. (2015) TLR4 expression in bone marrow-derived cells is both necessary and sufficient to produce the insulin resistance phenotype in diet-induced obesity. *Endocrinology* **156,** 103–113 CrossRef Medline
45. Liu, A., Chen, M., Kumar, R., Stefanovic-Racic, M., O'Doherty, R. M., Ding, Y., Jahnen-Dechent, W., and Borghesi, L. (2018) Bone marrow lympho-myeloid malfunction in obesity requires precursor cell-autonomous TLR4. *Nat. Commun.* **9,** 708 CrossRef Medline
46. Kim, K. A., Gu, W., Lee, I. A., Joh, E. H., and Kim, D. H. (2012) High fat diet-induced gut microbiota exacerbates inflammation and obesity in mice via the TLR4 signaling pathway. *PLoS One* **7,** e47713 CrossRef Medline
47. Caesar, R., Tremaroli, V., Kovatcheva-Datchary, P., Cani, P. D., and Bäckhed, F. (2015) Crosstalk between gut microbiota and dietary lipids aggravates WAT inflammation through TLR signaling. *Cell Metab.* **22,** 658–668 CrossRef Medline
48. Davis, J. E., Braucher, D. R., Walker-Daniels, J., and Spurlock, M. E. (2011) Absence of Tlr2 protects against high-fat diet-induced inflammation and results in greater insulin-stimulated glucose transport in cultured adipocytes. *J. Nutr. Biochem.* **22,** 136–141 CrossRef Medline
49. Ehses, J. A., Meier, D. T., Wueest, S., Rytka, J., Boller, S., Wielinga, P. Y., Schraenen, A., Lemaire, K., Debray, S., Van Lommel, L., Pospisilik, J. A., Tschopp, O., Schultze, S. M., Malipiero, U., Esterbauer, H., *et al.* (2010) Toll-like receptor 2-deficient mice are protected from insulin resistance and β cell dysfunction induced by a high-fat diet. *Diabetologia* **53,** 1795–1806 CrossRef Medline
50. Schuettpelz, L. G., and Link, D. C. (2013) Regulation of hematopoietic stem cell activity by inflammation. *Front. Immunol.* **4,** 204 Medline
51. Morris, M. C., Gilliam, E. A., and Li, L. (2014) Innate immune programing by endotoxin and its pathological consequences. *Front. Immunol.* **5,** 680 Medline
52. Shindou, H., Ishii, S., Yamamoto, M., Takeda, K., Akira, S., and Shimizu, T. (2005) Priming effect of lipopolysaccharide on acetyl-coenzyme A:lyso-platelet-activating factor acetyltransferase is MyD88 and TRIF independent. *J. Immunol.* **175,** 1177–1183 CrossRef Medline
53. Deng, J. C., Cheng, G., Newstead, M. W., Zeng, X., Kobayashi, K., Flavell, R. A., and Standiford, T. J. (2006) Sepsis-induced suppression of lung innate immunity is mediated by IRAK-M. *J. Clin. Invest.* **116,** 2532–2542 Medline
54. Morris, D. L., Oatmen, K. E., Wang, T., DelProposto, J. L., and Lumeng, C. N. (2012) CX3CR1 deficiency does not influence trafficking of adipose tissue macrophages in mice with diet-induced obesity. *Obesity* **20,** 1189–1199 CrossRef Medline
55. Lumeng, C. N., DelProposto, J. B., Westcott, D. J., and Saltiel, A. R. (2008) Phenotypic switching of adipose tissue macrophages with obesity is generated by spatiotemporal differences in macrophage subtypes. *Diabetes* **57,** 3239–3246 CrossRef Medline
56. Pronk, C. J., Rossi, D. J., Månsson, R., Attema, J. L., Norddahl, G. L., Chan, C. K., Sigvardsson, M., Weissman, I. L., and Bryder, D. (2007) Elucidation of the phenotypic, functional, and molecular topography of a myeloerythroid progenitor cell hierarchy. *Cell Stem Cell* **1,** 428–442 CrossRef Medline
57. Oguro, H., Ding, L., and Morrison, S. J. (2013) SLAM family markers resolve functionally distinct subpopulations of hematopoietic stem cells and multipotent progenitors. *Cell Stem Cell* **13,** 102–116 CrossRef Medline
58. Erickson, J. C., Clegg, K. E., and Palmiter, R. D. (1996) Sensitivity to leptin and susceptibility to seizures of mice lacking neuropeptide Y. *Nature* **381,** 415–421 CrossRef Medline